Understanding cyclic seismicity and ground deformation patterns at volcanoes: intriguing lessons from Tungurahua volcano, Ecuador

Jürgen W. Neuberg*[a], Amy S. D. Collinson[a], Patricia A. Mothes[b], Mario, C. Ruiz[b] and Santiago Aguaiza[b]

[a] School of Earth & Environment, The University of Leeds, Leeds, United Kingdom

[b] Instituto Geofisico, Escuela Politécnica Nacional, Quito, Ecuador

* Corresponding author E-mail address: j.neuberg@leeds.ac.uk

Cyclic seismicity and ground deformation patterns are observed on many volcanoes worldwide where seismic swarms and the tilt of the volcanic flanks provide sensitive tools to assess the state of volcanic activity. Ground deformation at active volcanoes is often interpreted as pressure changes in a magmatic reservoir, and tilt is simply translated accordingly into inflation and deflation of such a reservoir. Tilt data recorded by an instrument in the summit area of Tungurahua volcano in Ecuador, however, show an intriguing and unexpected behaviour on several occasions: prior to a Vulcanian explosion when a *pressurisation* of the system would be expected, the tilt signal declines significantly, hence indicating *depressurisation*. At the same time, seismicity increases drastically. Envisaging that such a pattern could carry the potential to forecast Vulcanian explosions on Tungurahua, we use numerical modelling and reproduce the observed tilt patterns in both space and time. We demonstrate that the tilt signal can be more easily explained as caused by shear stress due to viscous flow resistance, rather than by pressurization of the magmatic plumbing system. In general, our numerical models prove that if magma shear viscosity and ascent rate are high enough, the resulting shear stress is sufficient to generate a tilt signal as observed on Tungurahua. Furthermore, we address the interdependence of tilt and seismicity through shear stress partitioning and suggest that a joint interpretation of tilt and seismicity can shed new light on the eruption potential of silicic volcanoes.

Keywords

tilt; seismicity; eruption forecasting; shear stress; pressure; anti-correlation

1. Introduction

The combined monitoring of ground deformation and seismicity on active volcanoes provides one of the few direct links to the internal state of volcanic activity and its changes in near real-time. The identification of cyclic patterns in seismicity and deformation offers further insights regarding the temporal behaviour of a particular volcano and is essential to guide forecasting attempts. In many previous studies, surface deformation on active volcanoes has been inferred as caused by pressure changes within magmatic systems at depth (Anderson et al., 2010; Widiwijayanti et al., 2005). The tilt, defined as

$$\vartheta = \arctan\frac{dz}{dr} \qquad (1)$$

where *z* and *r* are the vertical and radial co-ordinates, respectively, is the change in inclination angle of the volcanic flanks, and is a particularly sensitive indicator of surface deformation. If tilt changes are modelled as caused by shallow, isotropic pressure sources with spherical or cylindrical geometries, they will often require unrealistically high overpressures, large conduit radii or extremely yielding material properties to reach high tilt amplitudes (Voight et al., 1999, 2010). Alternatively, elongated source bodies, such as dykes, can produce high tilt amplitudes in a zone located perpendicular to the strike of the dyke (Hautmann et al., 2009). In our modelling approach we will explore a set of isotropic pressure sources and a wide variety of material parameters and geometries in order to model the observed tilt patterns. An alternative mechanism pointing towards shear stress to generate high tilt amplitudes on volcanoes has been suggested by several studies. Beauducel et al. (2000) noted a striking link between seismicity - as a proxy for magma flux - and deformation. They suggested that the shallow deformation field on Merapi volcano, Indonesia, could be controlled by magma flux rather than by magma pressure variations. For Soufrière Hills volcano, Montserrat, during periods of rapid magma extrusion in 1997, we suggested changes in shear stress within the upper 1000 m of the magmatic system to explain the tilt amplitude of 20 μrad as an alternative to magma pressurisation (Green et al., 2006). Other examples using shear stress include Anderson et al. (2010), Albino et al. (2011), Costa et al. (2012), and Kawaguchi and Nishimura (2015).

In addition to the high tilt amplitudes, Tungurahua exhibits another striking feature concerning the timing of the tilt signal in relation to its volcanic activity; Vulcanian explosions are often - but not always - preceded by an increase in seismicity and a *decrease* in tilt, hence an apparent deflation of the edifice, or *depressurization* of the volcanic system several days before an eruption.

This intriguing pattern of seismicity, tilt and Vulcanian explosions has been observed on about 10 occasions, starting as early as 2006, (Fig 1) and has been utilised by scientists in charge of volcano monitoring in Ecuador in attempts in eruption forecasting. We investigate this pattern in a modelling approach, comparing quantitatively the traditional magma pressurization hypothesis with the effects of shear stresses along the conduit due to viscous flow resistance. We focus on periods associated with explosive activity in 2013 and 2014, which displayed strong surface deformation in the upper part of Tungurahua´s cone. The results demonstrate how much important information can be obtained from a single, strategically deployed tilt- and seismometer station, and how this can guide forecasting of the short-term eruption potential of Tungurahua.

2. Cyclic Deformation Associated with Vulcanian-Style Eruptions at Tungurahua 2013 - 2014.

Tungurahua volcano is an andesitic strato-volcano with historical eruptions ranging from 2 to 4 on the VEI scale. Its steep-sided, 3000 m relief cone has collapsed on several occasions and pyroclastic flows and ash falls are frequent hazards (Hall et al., 1999; Le Pennec et al., 2008). The present eruptive phase started in 1999 after nearly 80 years of repose (Mothes et al., 2015). Eruptions during the last 16 years have been accompanied by strong degassing (Hidalgo et al., 2014), long-period seismic activity (Kim et al., 2014), notable infrasound signals (Fee et al., 2013; Mothes et al., 2015) and ground deformation (Biggs et al., 2010; Champenois et al., 2014). We base our study on the tilt cycles and seismicity associated with four eruptive periods: three Vulcanian eruptive events on 14 July 2013, 18 October 2013 and 1 February 2014, and a fourth episode on 4 April 2014 involving both Strombolian and Vulcanian-style activity.

Deformation data are obtained from an electronic tilt meter at station RETU, located at 3950m elevation on the northern flank of the volcano, 2000 m north, and 1000 m below the summit vent (Fig. 2). The RETU tilt meter is a dual-axial platform analogue-output, model AGI, 711-2A series, with a 1 µrad resolution.

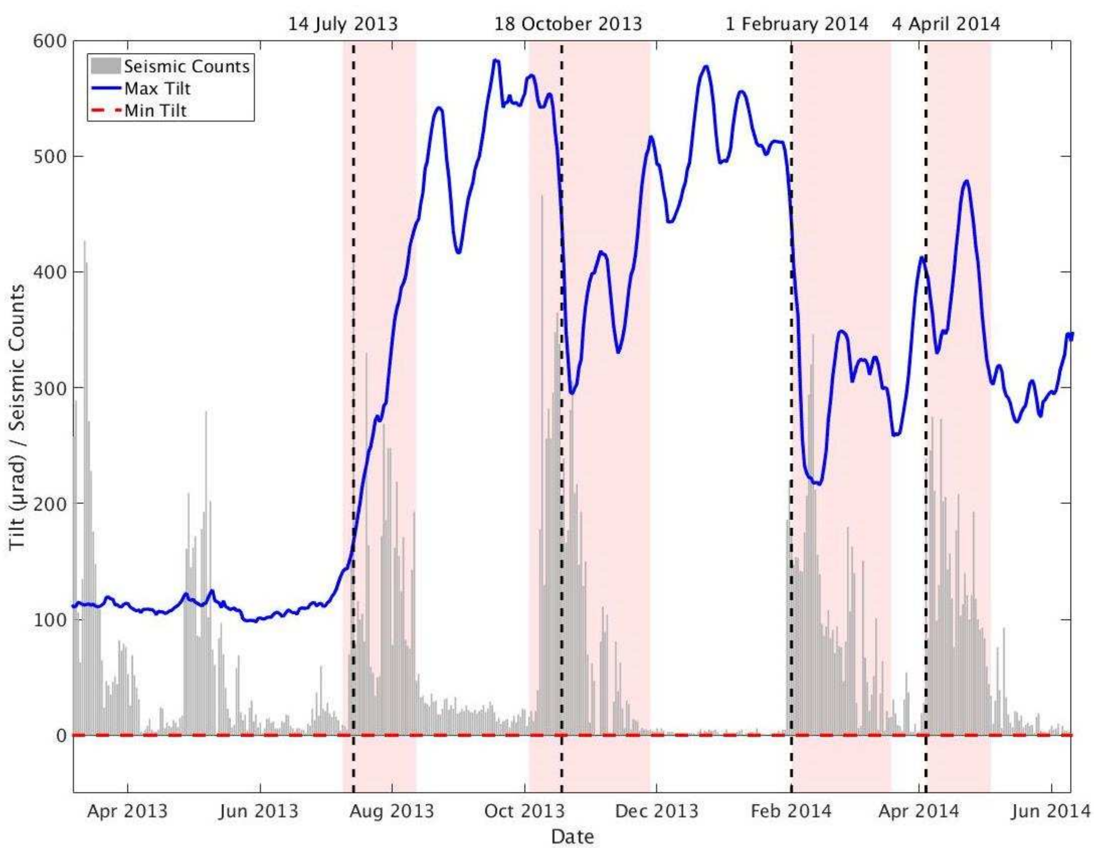

Figure 1: Daily averaged tilt (μrad) and daily event rate of long-period earthquakes recorded at RETU. East and North tilt components are rotated into the direction of maximum and minimum tilt plotted here, maximum tilt is used for further analysis. The four Vulcanian eruptions of interest are indicated (dashed lines) along with the associated eruptive phases (shaded) and described in the text. Note the remarkable magnitude of the maximum tilt. See the supplementary material for a zoomed view into the last three events Fig. S1.

It is anchored to a massive lava flow and buried in an insulated barrel that minimizes diurnal temperature changes. Data are recorded every 5 minutes and sent via analogue radio to the Tungurahua Volcano Observatory where they are decimated and stored in daily files. Several other continuously recording tilt meter stations are located lower on the volcano's flanks (Fig. 2) and have similar instrumentation, data recording and transmitting procedures. However, due to the larger distance from the conduit, these stations have been less sensitive to movements near the vent and conduit.

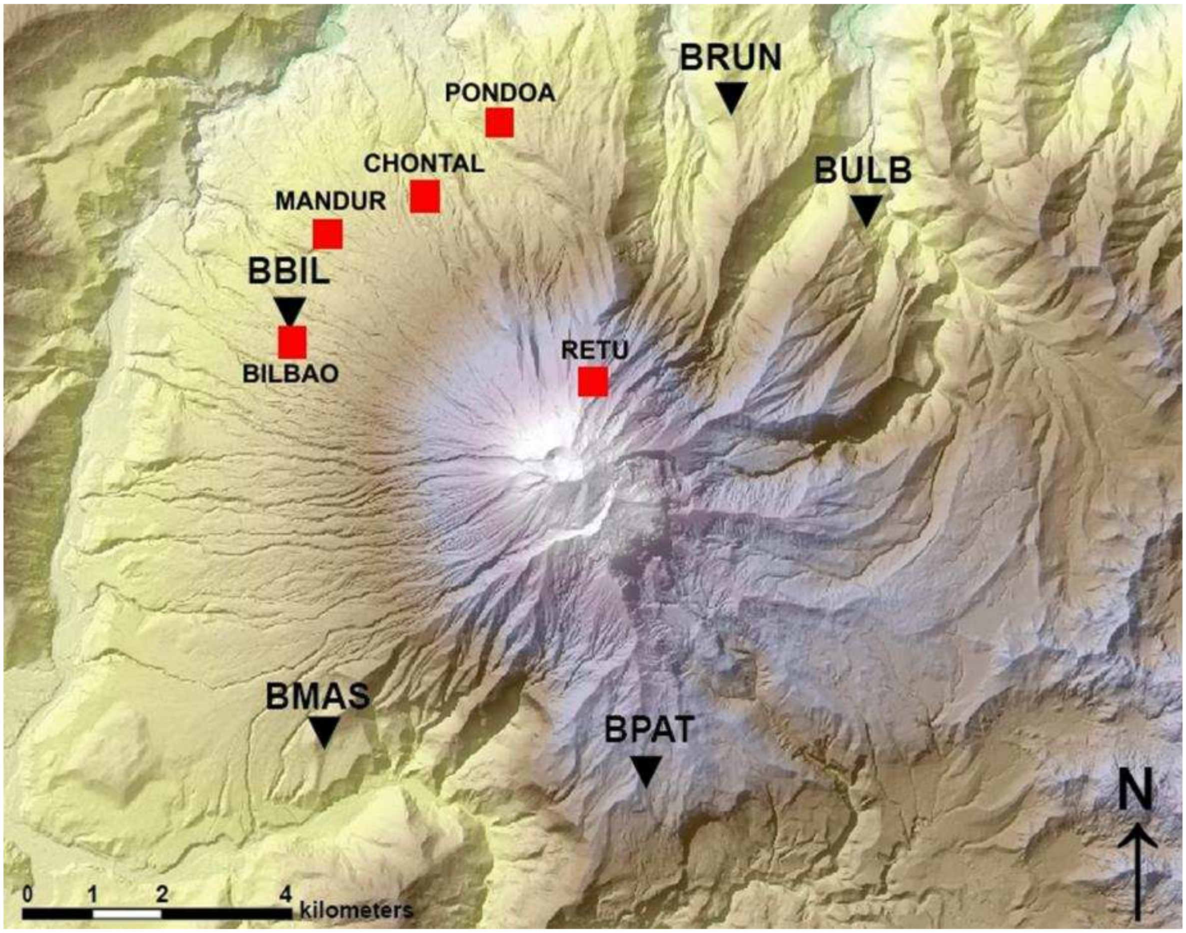

Figure 2: The seismic-acoustic (triangles) and deformation (squares) network at Tungurahua Volcano. RETU is also equipped with a short-period seismometer.

There is little apparent evidence for correlation between the data patterns at these distal sites with pre- and co-eruptive seismic patterns and explosive events. Therefore, in this study, we concentrate on the data from the RETU station comprising a tilt meter and a short-period seismometer.

For the current study, we use daily averaged tilt data and seismic counts recorded at RETU station. A higher resolution tilt record shows only the usual temperature dependent, small daily fluctuations, which are not relevant for the overall tilt behaviour. East and North tilt components are rotated into the direction of maximum tilt which is then used for further analysis. In contrast to other studies, we prefer to derive the direction of tilt from the data rather than assigning an assumed source location and splitting the data into “radial” and “tangential” components. Note that the back-azimuth derived from the maximum tilt does not necessarily point to the location of the deformation source, as it may be biased by topography. This bias is taken into account in our numerical model results by employing a high-resolution digital elevation model.

For at least 2 years prior to the first eruptive event of our study (14 July 2013), the tilt followed a fairly unremarkable, linearly increasing trend of approx. 100 µrad over two years with small oscillations of up to 10 µrad. The tilt behaviour prior to this period is not known. A sharp increase began in mid-June 2013 accompanied by the occurrence of 24 VT seismic events between 1 June and 13 July 2013. The accumulated tilt in the two weeks leading up to the 14 July 2013 eruption amounts to 60 µrad, which is significantly higher than the background trend of the previous 2 years. In the 12 hours prior to the explosion, the RETU seismic station recorded 332 low-amplitude LP seismic events, in comparison to the 641 events recorded in the previous 6 weeks. Furthermore, 3800 LP earthquakes occurred in the month following the main Vulcanian event. A typical example of seismic swarms recorded at RETU is depicted in the supplementary material Fig. S2.

While this initial event was preceded and accompanied by increased seismicity, there was no associated decrease in tilt. Following the explosion, the tilt at RETU continued to increase, resulting in an accumulated tilt of 440 µrad over 2 months, thereby marking the beginning of a remarkable tilt cycle and seismic pattern which is the main focus of this study.

Each of the following three events were preceded by increased seismicity, and the onset of a downward trending tilt 2-6 days prior to the eruption. In the case of the 18 October 2013 eruption, seismic counts increased significantly 10 days before the eruption occurred. The onset of increased seismicity coupled with the downward trending tilt allowed scientists from the Instituto Geofisico, Ecuador, responsible for the monitoring of Tungurahua, to provide a warning 36 hours before the explosive event of 1 February 2014.

The latter three events were followed by continued, decreasing tilt lasting 5-12 days after the explosive episode, and lingering seismicity. The elevated seismicity continued for 1-2 months after the eruptive events, before returning to the background level of up to six events per day.

In the event of 4 April 2014, the accumulated tilt and consecutive decrease were not as extreme with a drop of only 77 µrad, compared to 262 µrad and 302 µrad for the 18 October 2013 and 1 February 2014 events, respectively (Fig. 1).

All of the eruptive events involved modest Vulcanian explosions with ash ejected up to 10 km above the active vent, and associated pyroclastic flows went down the western flank of the volcano. Metre-sized bombs were ejected up to 4km from the vent, with some landing very close to the Pondoa community, located NW of the vent (Fig. 2).

3. Numerical Modelling of the Tilt Meter Data

We use the finite element software COMSOL Multiphysics 5.2 to construct a set of models investigating the deformation field at Tungurahua associated with changes in the stress tensor, either by pressure sources or shear stress. This approach allows us to consider simultaneously source processes, and the response of the elastic medium as well as topographic effects at several tilt meter sites on Tungurahua. Scenarios we consider include pressurisation of magma reservoirs with elliptical and cylindrical geometry, as well as ascending magma exerting both pressurisation and shear stress across the conduit wall. A Digital Elevation Model (DEM) of the edifice and surrounding area with a coverage of approx. 16 x 16 x 10 km and a resolution of 10 m is used (Fig. 3). Into this geometry different sources are inserted and modelled as voids in order to decrease the number of triangular and tetrahedral mesh elements. For topographical details and the region immediately surrounding the sources a finer mesh is used to ensure the accuracy of the results in the immediate area of interest. Mesh element size increases with depth and with lateral distance from the conduit. The largest model is run with a minimum element size of 5 m and a total of 240,000 elements resulting in 6 million degrees of freedom.

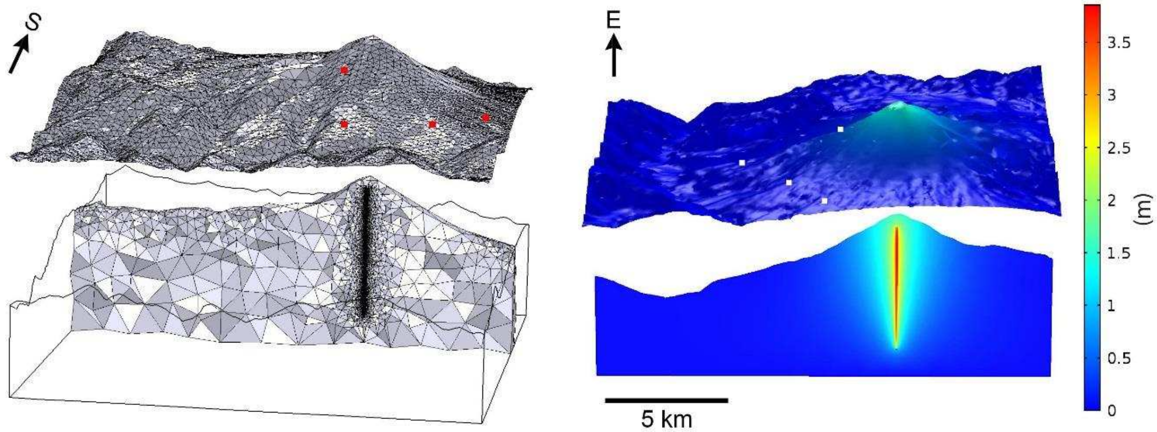

Figure 3: (left) Tungurahua model and mesh geometry and (right) Digital Elevation Model used with a cross-section through the conduit. View looking East, with the locations of four tilt meter stations marked by white/red dots; RETU closest to the volcanic summit and the distal stations of PONDOA, MANDUR and BILBAO (E – W). Colouration depicts the shear stress induced displacement in metres for a 4.5 km long conduit coinciding with maximum tilt. Note the different orientation right and left to show mesh at tilt sites and site locations more clearly.

The exterior lateral boundary conditions of the modelled geometry are set to “roller” which allows only vertical motion at the boundary; the basal boundary is fixed. To induce deformation the boundary conditions at the conduit source are set to either normal stress representing pressure or vertical shear stress. We introduce two types of time-dependence in our models: (i) For simulating an ascending magma column within the conduit, we apply constant pressure or shear stress to the growing length of the magma column that propagates from depth towards the surface with a constant magma ascent velocity. This creates an evolving deformation field of a moving source with constant amplitude. (ii) In contrast, to simulate a stationary source, we apply pressure and shear stress to the entire conduit from depth to surface, but vary the amplitude with time. This model simulates on the one hand a pressurisation of an emplaced magma column, or, on the other, variations in shear stress due to velocity or viscosity changes, applied to the entire magma column.

We simplify the potentially rather complex setting by modelling the volcanic edifice as homogeneous with a Poisson's ratio of 0.25. We consider variations in Young's modulus, conduit radius, stress magnitude, as well as extent and position of the source region.

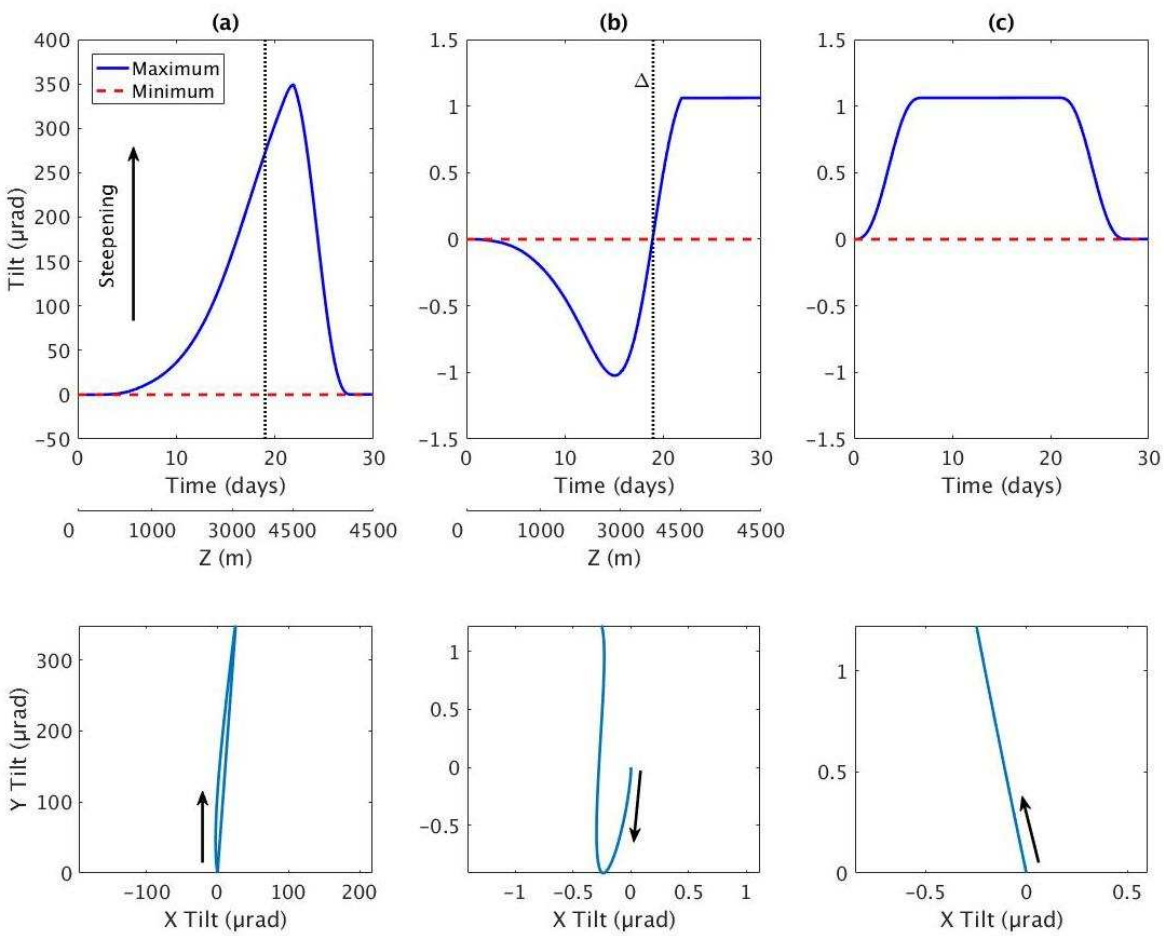

Figure 4: Results for three model runs with a conduit radius of 15 m, shear stress or pressure magnitude of 20 MPa along a conduit length of 4.5km, where Z indicates elevation. (a) ascending magma exerting shear stress along the conduit-wall boundary, (b) ascending and pressurising magma, and (c) pressurisation of a filled conduit. Tilt has been converted to maximum and minimum where the vertical line marks the elevation of the tilt meter (Top). The trajectory of the tilt meter for each scenario is also shown (Bottom).

Our initial numerical models without topography have been benchmarked against analytical solutions for spherical chamber models, dykes and cylindrical conduits provided by Segall (2010). This enabled us to ascertain the optimum model set-up and ensure that the tilt meter locations are sufficiently distant from the exterior model boundaries such that their effect on the results is negligible.

The modelling results for Tungurahua tilt meter RETU are depicted in Figure 4. In general, the tilt amplitude is dependent upon source location and size, material properties (Young's modulus) and applied stress (pressure vs. shear stress). In the following we discuss the impact of these factors on the observed tilt signal on Tungurahua.

We find that a shear stress of 20 MPa is sufficient to explain the tilt of up to 480 µrad (Fig 4a) for a conduit radius of 15 m and Young's modulus of 1 GPa. However, a conduit pressure of several hundreds of MPa is required to reach the observed tilt. At shallow depths within the volcano, such high pressurisation would exceed the mechanical strength of any rock. Unsurprisingly, the results for a conduit with a 15 m radius that is pressurized by 20 MPa fail to explain the observations by two orders of magnitude (Fig. 4b and c).

With a Young's modulus of 1GPa (e.g. Young & Gottsmann, 2015) we assume a low rigidity representing the upper part of the volcanic edifice probably weakened by hydrothermal activity and fractured rocks. Lowering Young's modulus by another order of magnitude would still result in unrealistically high pressures necessary to explain the tilt amplitude. For a 15 m conduit and a pressurisation of 20 MPa, a Young's modulus as low as 10^{-3} GPa would be required to explain the tilt magnitudes observed at Tungurahua. Even though the tilt meter is at a horizontal distance of 2000 m away from the conduit, one could argue that the entire upper edifice is fractured and incoherent to such a degree that the elastic rheology we use should be replaced by inelastic or plastic behaviour. However, the fast recovery and rebound of the edifice argues against this suggestion.

The ascending magma column (Fig. 4b) induces negative tilt as long as magma ascends below the tilt station and only steepens the flank (positive tilt) once the top of the magma column has exceeded the tilt meter elevation. If we used a more realistic magma-static pressure in addition to the uniformly applied constant pressure, most of the pressurisation would be exerted below the tilt station, hence, increasing the negative tilt amplitude. The non-linear trajectory of ground motion (Fig 4b, bottom) is due to topography and does not occur in a radially symmetric cone model. If an elongated pressure source of large dimensions (e.g. 100 x 700 m) is employed with the longer axis exactly perpendicular to the radial (maximum) tilt direction, the model provides amplitudes similar to the observation, and will show a linear trajectory of particle motion during a tilt cycle. If the tilt meter is deployed at any other angle relative to the elongated source the deformation will show a curved trajectory, resulting in both radial and tangential tilt components (Hautmann et al., 2009). This is only the case for elongated, pressurized sources, or due to topography (Fig. 4b) but not for tilt caused by shear stress (Fig. 4a). Therefore, when combined with other data the tilt trajectory may be useful to discriminate between the different source processes, either elongated pressure source or shear stress across the conduit wall. Considering that the East and North component of the RETU tilt station display a perfectly linear trajectory (see Figure S7, supplementary material), the direction of which we refer to as the maximum tilt component, and given the high tilt amplitude, we suggest the tilt at RETU is not a result of an elongated, pressurized conduit.

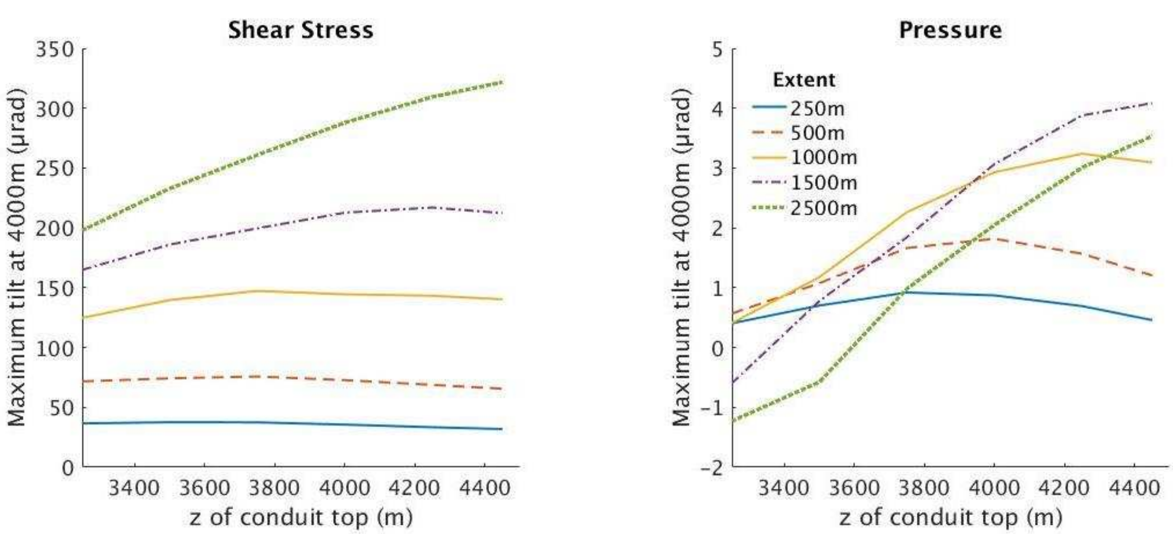

Figure 5. Maximum tilt modelled at RETU for localised pressure (right) and shear stress sources (left) of varying conduit length and its upper limit elevation z. Models are

stationary and vary between 250 m and 2500 m in conduit length. The tilt meter is located at z = 4000 m. Note that pressurisation leads to mainly horizontal deformation while shear stress results in vertical deformation which is dependent on the integral over the conduit length affected by the shear stress. Small negative tilt values are generated in the models by pressurising the edifice below the tilt meter station.

Assuming a conduit pressure of 20 MPa with a conduit radius of 15 m and Young's modulus of 1 GPa, the maximum tilt reaches only 1.5 µrad. In contrast, a variety of shear stress locations and extents are capable of generating the required tilt. A conduit radius of 100 m would generate only 60 µrad of tilt in response to 20 MPa pressure. A pressure source with a significantly larger radius of a few hundred meters would produce an increased tilt amplitude (see supplementary material Fig. S3). However, our modelling shows that the pressure source needs to be located above the level of the tilt meter station in order to show high, positive tilt amplitudes (Fig 5). Such an extended source in the upper part of the volcanic edifice seems to be very unlikely. Therefore, we use a conduit radius of 15 m (Mothes et al, 2015) in the models presented in this study. This is in agreement with Ruiz et al. (2006) who estimated a conduit radius of approximately 10 m based on FLIR images of the Tungurahua vent in March 2003 taken by Samaniego et al. (2003).

In summary, large, shallow over-pressurization can be a natural consequence of higher viscosities at the conduit top, however even a large overpressure is not large enough to produce the observed tilt signal. In order to explain the tilt signal by a pressurised conduit, either unrealistically high pressures, or extremely weak material, or a huge conduit would have to be assumed as listed in Table 1.

Young's Modulus (GPa)	**Radius (m)**	**Pressure (MPa)**	**Tilt (µrad)**
1	15	400	350
10^{-3}	15	20	350
1	100	20	60
1	500	20	350
Young's Modulus (GPa)	**Radius (m)**	**Shear Stress (MPa)**	**Tilt (µrad)**
10	15	200	350
1	15	20	350

Table 1. Combinations of Young's modulus, conduit radius and pressure/shear-stress required to simulate the tilt signal of 350 µrad measured at the station RETU.

Nevertheless, one could argue that shear stress is not necessarily the only explanation for the observed tilt signal. However, our numerical modelling explained in the next section demonstrates that shear stress provides the *sufficient condition* for the observed deformation field. Realistic magma viscosity values of around 10^{11} Pas and ascent rates as low as of $0.0015 ms^{-1}$ will result in a shear stress of 20 MPa at the conduit wall. And shear stress of that magnitude will result in a deformation field that is observed as tilt on nearby tilt stations. Hence, for RETU, located at a horizontal distance of 2000m from the conduit, shear stress provides the most suitable explanation for the strong deformation. The lower elevation tilt meter stations of PONDOA, MANDUR and BILBAO (Fig 2 and supplementary material Fig. S4) display only minor deformation compared to RETU, which is also corroborated through our modelling results (supplementary material Fig S5). This fact suggests that shear stress as a deformation source is only applicable for monitoring sites proximal to the uppermost 1000 m of the conduit where the shear stress originates from ascending magma and its traction along the conduit-wall boundary. Hence, shear stress as a deformation source is not at all unique to Tungurahua volcano but should be considered for other silicic systems. It is the proximity of the tilt meter site to the conduit that plays the deciding role which dominant source process causing the deformation field is observed. This has important implications for monitoring strategies and the selection of suitable sites for tilt meters.

4. Discussion

Assuming that the preferred source mechanism for the tilt cycles on Tungurahua is explained by shear traction across the conduit wall, which is counteracted by elastic deformation of the surrounding edifice and gravity, we shall shed some further light on the fundamental processes that govern the generation of the shear stress due to viscous magma flow.

For Newtonian flow, the vertical shear stress σ is given by

$$\sigma = \frac{d\varepsilon}{dt}\,\mu = \frac{dV}{dr}\,\mu \tag{2}$$

where μ is the magma viscosity, $d\varepsilon/dt$ is the shear strain rate, which equals dV/dr , the lateral gradient of the magma ascent velocity across the conduit (Neuberg et al., 2006). Hence, variations in shear stress resulting in tilt changes can be caused by either temporal or spatial magma viscosity changes as magma ascends, or simply by variations in magma ascent velocity.

In the following we test if magma viscosity, shear stress at the conduit wall and ascent rate are in the right ballpark. We consider velocity changes and estimate the shear stress at the conduit wall for a given radius and magma ascent velocity. Assuming a constant magma viscosity across the conduit, the velocity for ascending magma is given by the Hagen–Poiseuille flow, showing a parabolic velocity profile, $V \sim r^2$,

$$V = \frac{1}{4\mu} \quad \frac{\Delta P}{\Delta z} \quad (R^2 - \ r^2) \tag{3}$$

with conduit radius R. The ascent velocity at the centre of the conduit $r = 0$ is

$$V_{max} = \frac{1}{4\mu} \quad \frac{\Delta P}{\Delta z} \ R^2 \tag{4}$$

hence, using eq 3 and 4 the strain rate at the conduit wall ($r = R$) is given by

$$\frac{dV}{dr} \Big|_{r=R} = -2 \frac{V_{max}}{R} \tag{5}$$

where the shear stress is

$$\sigma = \ 2 \ \mu \frac{V_{max}}{R} \, . \tag{6}$$

Using the petrological analysis for andesite erupted in 2006 from Tungurahua (Samaniego et al., 2011) in the viscosity calculator of Giordano et al. (2008), we estimate, for the degassed upper conduit, a melt viscosity range of 10^8-10^{10} Pas. Taking crystallinity into account and assuming a magma viscosity of 10^{11} Pas, a shear stress of 20MPa along the conduit wall, which is consistent with the observations, can be generated by an ascent rate as low as 0.0015 ms^{-1}.

In addition to all the considerations given to the high tilt amplitude, the time history of the RETU tilt record with respect to the Vulcanian explosion provides another clue as to the origin of the deformation. It is hard to imagine that the volcanic plumbing system depressurizes just a few days prior to a VEI 2 or 3 eruption. However, if interpreted as an ascending magma column where tilt is caused by shear stress exerted along the entire conduit, an ascending magma batch that encounters increased friction at the limited section of the degassed top of the conduit will slow down the entire magma column. At Tungurahua, numerous microlites are present within the eruptive products of July and October 2013, and February 2014 (Gaunt et al., 2015). This is a strong indication that with decreasing temperature and increasing crystal load, the magma viscosity and, therefore, shear resistance will increase in the upper conduit. This will result in a decrease in the tilt amplitude, which is proportional to the magma ascent velocity of the entire magma column.

The tilt signal is generated by the superposition of the shallow section with increased shear stress and by traction along the entire conduit where slowing ascent velocity leads to decreasing shear stress. Hence, as shown in Figure 5 the entire conduit dominates the final tilt amplitude, rather than the limited zone where seismicity is generated. With increasing viscosity, generated by a higher proportion of crystals the magma column slows down, and so does the tilt amplitude.

While the overall tilt signal remains positive, the lower shear stress allows the elastic and gravitational rebound of the edifice, hence a decrease in the tilt amplitude. As seen in our modelling, a negative tilt signal could only be produced by viscous magma descending the conduit, or by unrealistically high overpressure acting below the altitude of the tilt meter site.

Several undulations in the tilt behaviour (Fig 1, supplementary material Fig S5)) can, therefore, likely be attributed to changes in magma ascent velocities. Following a more drastic decrease in magma ascent velocity, the subsequent local pressurization by a few tens of MPa in the upper portion of the conduit (Sparks, 1997) will lead to the Vulcanian explosion. High internal pressure gradients are also evidenced by the remarkable infrasound values of these explosions and by the ballistic ejection of metre-sized rocks up to 4 km distance (Fee and Matoza, 2013; Mothes et al, 2015). However, as our modelling has shown, even such high pressurization of the upper conduit would not translate into a significant tilt signal at RETU.

The long-period (LP) seismicity observed on the RETU seismometer (Fig 1) during these episodes points to a viscous-brittle transition of the crystal rich magma. In general, LP earthquakes are triggered by shear failure. Two end-member models use either stick-slip motion (Iverson et al., 2006) or brittle failure in the magma near the conduit wall where the strain rate is highest (Neuberg et al., 2006). In both cases shear stress across the conduit wall will drop by the amount used to generate the seismicity, and tilt will decrease accordingly. Such anti-correlated behaviour between LP seismicity and tilt was noted by several studies on Soufrière Hills volcano, Montserrat (Neuberg et al., 2006; Voight et al., 1998), however, without explaining the causal link. During each tilt cycle on Soufrière Hills, both the beginning and end of a period of seismicity coincided with a curvature change in the tilt signal. This indicates the interference of competing physical processes. Shear stress partitioning between the generation of seismicity on the one hand, and surface deformation and tilt on the other can explain this observation. On Tungurahua, we observe a very similar, anti-correlated behaviour associated with the Vulcanian explosions. However, conditions seem to be different for the first and most violent explosion on 14 July 2013, which initiated the transition to increased volcanic activity. We speculate that the first explosion was a consequence of a pressurised magma body that was already emplaced. The small tilt signal preceding the explosion indicates little upward magma motion accompanied by accelerating seismic LP swarms as the magma plug with high crystallinity is forced out. With a seismic network denser than that on Tungurahua, one could also obtain precise locations of the LP swarms, constraining the migration of the magma plug.

The seismic signature of accelerating LP occurrence (see supplementary material Fig S6) is typical in preceding events like explosions or lava dome collapses (Hammer and Neuberg, 2006; De la Cruz-Reyna et al., 2001). The explosion evacuates large parts of the conduit which is then refilled by buoyant, new magma, the ascent of which produces a strong increase in tilt, a behaviour repeated after each subsequent explosion.

5. Conclusion

We have demonstrated through a set of numerical models that the strong tilt signal recorded close to the magma conduit of Tungurahua can be most realistically explained by shear stress exerted by magma movement rather than by pressurization of a magma body. Some unrealistic input values for conduit radius, Young's modulus or pressure are required in the modelling to match the tilt observations. While using shear stress as a deformation source does not constitute a necessary condition, it is sufficient to explain the tilt observations: we have demonstrated that magma with a representative viscosity and ascent rate will yield a realistic shear stress that is capable of generating the observed tilt signal. This alternative interpretation of monitoring data is essential as it replaces the more traditionally assumed *inflation* of a magma body through *magma ascent*, and more importantly, explains why the assumed *deflation* is not necessarily caused by depressurization, but rather by a *decrease in shear stress* and resumption of elastic and gravitational rebound of the edifice. For Tungurahua, this interpretation also explains the intriguing timing of alleged deflation prior to Vulcanian explosions. We explain the cyclic tilt behaviour by changes in magma ascent velocity. After each explosive episode fresh magma ascends exerting shear stress along the conduit wall inducing surface deformation and tilt. The entire ascending magma column slows down when viscosity increases due to crystallisation in the upper conduit. This decrease in ascent velocity causes the corresponding drop in tilt amplitude. Seismicity is generated where magma goes through the ductile- brittle transition, and shear stress drops further by the amount dedicated to the generation of this seismicity. This leads to an anti-correlated behaviour between seismicity and tilt as evidenced by the observations.

The strategic deployment of a tilt meter high up on the edifice, and close to a magma conduit combined with any seismic monitoring tool offers the possibility to obtain essential parameters for short-term volcano forecasting from a minimal instrumental set-up. Both Tungurahua and Soufrière Hills demonstrate the importance of such a joint interpretation due to the anti-correlated relationship between seismicity and tilt amplitude, i.e. seismicity increases while tilt decreases. This suggests shear stress partitioning between the two competing processes. Based on the interpretation of tilt as caused by shear stress generated by magma tracking up the conduit, and seismicity as a consequence of stick-slip or brittle failure, both of these two processes point towards magma ascent in the last few hundreds of meters below the conduit top. Hence, combining tilt and seismicity can give a quantitative measure of magma ascent rate. However, the exact partitioning of shear stress also depends on magma properties such as yield strength and viscosity. Non-Newtonian behaviour and shear thinning will also affect shear stress in the upper conduit, and therefore provide a further contribution to the tilt signal (Caricchi et al., 2007; Costa, 2005). Shear heating in parts of the conduit might play an important role in the viscosity distribution and the resulting shear stress along the conduit wall. Further studies into temperature- and strain rate-dependent magma viscosity will help to constrain our models of magma ascent rate which is the critical parameter that controls the eruption style: lower ascent rates lead to effusive magma extrusion while fast rates can result in explosive behaviour that generates heightened levels of hazards. Hence, being able to estimate the magma ascent rate will increase the chances of early warning.

Acknowledgements:

We would like to thank the IGEPN staff for keeping all monitoring operations on Tungurahua optimally functioning, as well as the rotating OVT staff who foster data reception and facilitate communication and early warnings. ASDC and JWN are partly funded by NERC/ESRC project “Strengthening Resilience in Volcanic Areas” (STREVA), the European Union Framework Program 7 Grant 739 282759 (VUELCO), as well as the Centre for the Observation and Modelling of Earthquakes, Volcanoes and Tectonics (COMET). Yan Lavallée, Paul Segall and Marie Edmonds are acknowledged for insightful discussions on this topic. Luke Marsden has provided figures for the supplementary material. Finally we would like to thank Jackie Kendrick and one anonymous reviewer for providing us with helpful and constructive comments and suggestions.

References:

Anderson, K., Lisowski, M., Segall, P., 2010. Cyclic ground tilt associated with the 2004–2008 eruption of Mount St. Helens. J. Geophys. Res. 115, B11201, doi: 10.1029/2009JB007102.

Beauducel, F.,Cornet, F.-H., Suhanto, E., Duquesnoy, T., Kasser, M., 2000. Constraints on magma flux from displacements data at Merapi volcano, Java, Indonesia. J. Geophys. Res. 105 (B4), 8193–8203, doi: 10.1029/1999JB900368.

Biggs, J., Mothes, P., Ruiz, M., Amelung, F., Dixon, T.H., Baker, S., Hong, S.-H., 2010. Stratovolcano growth by co-eruptive intrusion: The 2008 eruption of Tungurahua Ecuador. Geophys. Res. Lett. 37 (21), L21302, doi: 10.1029/2010GL044942.

Caricchi, L., L. Burlini, P. Ulmer, T. Gerya, M. Vassalli and P. Papale, 2007. Non-Newtonian rheology of crystal-bearing magmas and implications for magma ascent dynamics. Earth Planet. Sci. Lett., 264: 402-419.

Champenois, J., Pinel, V., Baize, S., Audin, L., Jomard, H., Hooper, A., Alvarado, A., Yepes, H., 2014. Large-scale inflation of Tungurahua volcano (Ecuador) revealed by Persistent Scatterers SAR interferometry. Geophys. Res. Lett. 41, 5821–5828, doi: 10.1002/2014GL060956.

Costa, A. ,2005. Viscosity of high crystal content melts: Dependence on solid fraction. Geophys. Res. Lett. 32 (22), L22308.

De la Cruz-Reyna, S., Reyes-Dávila, G.A., 2001. A model to describe precursory material failure phenomena: applications to short-term forecasting at Colima Volcano, Mexico. Bull. Volcanol. 63 (5), 297–308.

Fee, D., Matoza, R.S., 2013. An overview of volcano infrasound: From hawaiian to plinian, local to global. J. Volcanol. Geotherm. Res. 249, 123-139, doi: 10.1016/j.volgeores.2012.09.002.

Gaunt, E., Mothes, P., Chadderton, A., Lavallee, Y. 2015. Physical characteristics of conduit plug rocks during Vulcanian eruptions at Cotopaxi and Tungurahua volcanoes, Ecuador. IUGG General Assembly, Prague Czech Republic, Abstract ID VS23p-586

Giordano, D., Russel, J.K., Dingwell, D.B., 2008. Viscosity of magmatic liquids: A model. Earth Planet. Sci. Lett. 271, 123-134, doi: 10.1016/j.epsl.2008.03.038.

Green, D.N., Neuberg, J., Cayol, V., 2006. Shear stress along the conduit wall as a plausible source of tilt at Soufrière Hills volcano, Montserrat. Geophys. Res. Lett. 33 (10), L10306, doi: 10.1029/2006GL025890.

Hall, M.L., Robin, C., Beate, B., Mothes, P., Monzier, M., 1999. Tungurahua Volcano, Ecuador: structure, eruptive history and hazards. J. Volcanol. Geotherm. Res. 91 (1), 1-21, doi: 10.1016/S0377-0273(99)00047-5.

Hammer, C; Neuberg, J.W., 2009. On the dynamical behaviour of low-frequency earthquake swarms prior to a dome collapse of Soufriere Hill volcano, Montserrat, Geophys. Res. Lett., 36 (6) L06305, doi:10.1029/2008GL036837

Hautmann, S., Gottsmann, J., Sparks, R.S.J., Costa, A., Melnik, O., Voight, B., 2009. Modelling ground deformation caused by oscillating overpressure in a dyke conduit at Soufrière Hills Volcano, Montserrat. Tectonophysics 471 (1-2), 87–95, doi: 10.1016/j.tecto.2008.10.021.

Hidalgo, S., Battaglia, J., Bernard, B., Steele, A., Arellano, S., Galle, B ., 2014. Identifying open and closed system behaviors at Tungurahua volcano (Ecuador) using SO2 and seismo-acoustic measurements. EGU General Assembly, Vienna Austria, Abstract id 1615541H.

Iverson, R.M., Dzurisin, D., Gardner, C.A., Gerlach, T.M., LaHusen, R.G., Lisowski, M., Major, J.J., Malone, S.D., Messerich, J.A., Moran, S.C., Pallister, J.S., Qamar, A.I., Schilling, S.P., Vallance, J.W., 2006. Dynamics of seismogenic volcanic extrusion at Mount St Helens in 2004–05. Nature 444, 439–443, doi: 10.1038/nature05322.

Kim, K., Lees, J.M., Ruiz, M.C., 2014. Source mechanism of Vulcanian eruption at Tungurahua Volcano, Ecuador, derived from seismic moment tensor inversions. J. Geophys. Res. 119 (2), 1145–1164, doi: 10.1002/2013JB010590.

Lavallée, Y., Dingwell, D.B., Johnson, J.B., Cimarelli, C., Hornby, A.J., Kendrick, J.E., von Aulock, F.W., Kennedy, B.M., Andrews, B.J., Wadsworth, F.B., Rhodes, E., Chigna, G., 2015. Thermal vesiculation during volcanic eruptions. Nature 528, 544-547, doi: 10.1038/nature16153.

Le Pennec, J.-L., Jaya, D., Samaniego, P., Ramon, P., Yanez, S.M., Egred, J., van der Plicht, J., 2008. The AD 1300-1700 eruptive periods at Tungurahua volcano, Ecuador, revealed by historical narratives, stratigraphy and radiocarbon dating. J. Volcanol. Geotherm. Res. 176, 70-81, doi: 10.1016/j.jvolgeores.2008.05.019.

Mothes, P.A., Yepes, H.A., Hall, M.L., Ramón, P.A., Steele, A.L., Ruiz, M.C., 2015. The scientific–community interface over the fifteen-year eruptive episode of Tungurahua Volcano, Ecuador. J. Applied. Volcanol. 4, 1-15, doi: 10.1186/s13617-015-0025-y.

Neuberg, J.W., Tuffen, H., Collier, L., Green, D., Powell, T., Dingwell, D., 2006. The trigger mechanism of low-frequency earthquakes on Montserrat. J. Volcanol. Geotherm. Res. 153 (1-2), 37–50, doi: 10.1016/j.jvolgeores.2005.08.008.

Ruiz, M.C., Lees, J.M., Johnson, J.B. 2006. Source constraints of Tungurahua volcano explosion events. Bull. Volcanol. 68 (5), 480-490, doi: 10.1007/s00445-005-0023-8

Samaniego, P., Eissen, J.-P., Le Pennec, J.-L., Hall, M., Monzier, M., Mothes, P., Ramón, P., Robin, C., Egred, J, Molina, I., Yepes, H. 2003. Los Peligros Volcánicos Asociados con el Tungurahua (in Spanish). Coporación Editora Nacional, IGEPN, IRD, Quito (2003) 180pp.

Samaniego, P., Le Pennec, J.-L., Robin, C., Hidalgo, S., 2011. Petrological analysis of the pre-eruptive magmatic process prior to the 2006 explosive eruptions at Tungurahua volcano (Ecuador). J. Volcanol. Geotherm. Res. 199, 69-84, doi: 10.1016/j.jvolgeores.2010.10.010.

Segall, P., 2010. Earthquake and volcano deformation, Princeton University Press, pp 200 – 254.

Sparks, R.S.J., 1997. Causes and consequences of pressurisation in lava dome eruptions. Earth Planet. Sci. Lett. 150 (3-4), 177–189, doi: 10.1016/S0012-821X(97)00109-X.

Sparks, R.S.J., Young, S.R., Barclay, J., Calder, E.S., Cole, P., Darroux, B., Davies, M.A., Druitt, T.H., Harford, C., Herd, R., James, M., Lejeune, A.M., Loughlin, S., Norton, G., Skerrit, G., Stasiuk, M.V., Stevens, N.S., Toothill, J., Wadge, G., Watts, R., 1998. Magma production and growth of the lava dome of the Soufrière Hills Volcano, Montserrat, West Indies: November 1995 to December 1997. Geophys. Res. Lett. 25 (18), 3421–3424, doi: 10.1029/98GL00639.

Voight, B., Hoblitt, R.P., Clarke, A.B., Lockhart, A.B., Miller, A.D., Lynch, L., McMahon, J., 1998. Remarkable cyclic ground deformation monitored in real-time on Montserrat, and its use in eruption forecasting. Geophys. Res. Lett. 25 (18), 3405–3408, doi: 10.1029/98GL01160.

Voight, B., Sparks, R.S.J., Miller, A.D., Stewart, R.C., Hoblitt, R.P., Clarke, A., Ewart, J., Aspinall, W.P., Baptie, B., Calder, E.S., Cole, P., Druitt, T.H., Hartford, C., Herd, R.A., Jackson, P., Lejeune, A.M., Lockhart, A.B., Loughlin, S.C., Luckett, R., Lynch, L., Norton, G.E., Robertson, R., Watson, I.M., Watts, R., Young, S.R., 1999. Magma Flow Instability and Cyclic Activity at Soufriere Hills Volcano, Montserrat, British West Indies. Science 283 (5405), 1138-1142, doi: 10.1126/science.283.5405.1138.

Voight, B., Hidayat, D., Sacks, S., Linde, A., Chardot, L., Clarke, A., Elsworth, D., Foroozan, R., Malin, P., Mattioli, G., McWhorter, N., Shalev, E., Sparks, R.S.J., Widiwijayanti, C., Clarke, A., Elsworth, D., Voight, B., 2005. Geodetic constraints on the shallow magma system at Soufrière Hills Volcano, Montserrat. Geophys. Res. Lett. 32 (11), L11309, doi: 10.1029/2005GL022846.

Widiwijayanti, C., Young, S.R., 2010. Unique strainmeter observations of Vulcanian explosions, Soufrière Hills Volcano, Montserrat, July 2003. Geophys. Res. Lett. 37 (19), L00E18, doi: 10.1029/2010GL042551.

Young, N. K., Gottsmann, J. 2015. Shallow crust mechanics from volumetric strain data: Insights from Soufrière Hills Volcano, Montserrat. J. Geophys. Res. Solid Earth, 120 (3), 1559-1571. Doi:10.1002/2014JB011551